# Dielectronic capture processes in highly charged uranium ions

M. S. Pindzola and N. R. Badnell
*Department of Physics, Auburn University, Auburn, Alabama 36849*
(Received 11 May 1990)

Dielectronic capture processes in highly charged uranium ions are studied in the isolated-resonance, distorted-wave approximation. A fully relativistic Dirac-Fock method is employed to calculate resonant transfer and excitation cross sections for collisions of $U^{90+}$ and $U^{89+}$ with $H_2$ and dielectronic recombination cross sections associated with the $2p \rightarrow 2s$ stabilizing transition of $U^{89+}$. A semirelativistic method based on the previously developed AUTOSTRUCTURE code is found to give cross sections in good agreement with the Dirac-Fock method in all cases. When the Dirac-Fock method is further extended to include the effect of the two-body Breit interaction, substantial changes are found in certain low-energy cross sections associated with $K$-shell resonant transfer and excitation, but little change is found in the $\Delta n = 0$ dielectronic recombination cross sections.

## I. INTRODUCTION

The advent of highly charged heavy-ion accelerators and storage rings has sparked renewed interest in relativistic atomic structure and dynamics.[1] There are two types of heavy-ion experiments currently evisaged which involve relativistic dielectronic capture processes. The first is a heavy-ion collision with a fixed atomic or molecular target,[2] while the second is a merged electron-ion beams collision.[3] Both involve the simultaneous capture of one electron by the ion and excitation of a second electron associated with the ion. The energy-specific resonant ionic state is detected by monitoring its characteristic x-ray emission or by counting the number of stable recombined ions. The theoretical calculations of the processes of resonant-transfer excitation followed by x-ray stabilization (RTEX) and dielectronic recombination (DR) are quite similar.[4,5]

In support of current heavy-ion experiments[2,3] we report on fully relativistic Dirac-Fock calculations for RTEX cross sections involving collisions of $U^{90+}$ and $U^{89+}$ with molecular hydrogen and DR cross sections associated with the $2p \rightarrow 2s$ stabilizing transition of $U^{89+}$. The fully relativistic method is based on the multiconfiguration Dirac-Fock approximation for atomic structures.[6] By modifying the program AUTOSTRUCTURE,[7,8] we also develop a semirelativistic method which provides RTEX and DR cross sections in good agreement with the Dirac-Fock method in all cases. The semirelativistic method allows rapid evaluation of DR and RTEX cross sections involving full Rydberg series. The Dirac-Fock method is further extended to include Breit interaction and QED effects on energies, wave functions, and transition amplitudes. Substantial changes are found in certain low-energy RTEX cross sections, but little change is found in the $\Delta n = 0$ DR cross sections. In Sec. II we outline the theory behind our calculations while in Sec. III we describe its application to RTEX and DR cross sections for highly ionized uranium. A brief summary is contained in Sec. IV.

## II. THEORY

In the isolated resonance approximation, the energy-averaged dielectronic recombination cross section for a given initial level $i$ through an intermediate level $j$ is given by[9]

$$\bar{\sigma}(i \rightarrow j) = \frac{\pi^2}{E_c \Delta E_c} \frac{g_j}{2g_i} \frac{A_a(j \rightarrow i) \sum_k A_r(j \rightarrow k)}{\sum_h A_a(j \rightarrow h) + \sum_h A_r(j \rightarrow h)} . \quad (1)$$

The above equation is in atomic units and $E_c$ is the energy of the continuum electron which is fixed by the position of the resonances, $\Delta E_c$ is a bin width, $g_j$ is the statistical weight of the $(N+1)$-electron doubly excited level, and $g_i$ is the statistical weight of the $N$-electron target level. The radiative $A_r$ and autoionization $A_a$ rates are evaluated using many-body perturbation theory, as described below.

Using the impulse approximation,[4,5] the total resonant-transfer excitation cross section for an initial level $i$ is given by

$$\sigma_{\mathrm{RTEX}}(i) = \sum_j F(Q) \bar{\sigma}(i \rightarrow j) \Delta E_c \left[ \frac{M}{2E} \right]^{1/2} , \quad (2)$$

where $F(Q)$ is the Compton profile[10] with

$$Q = \left[ E_c - \frac{Em}{M} \right] \left[ \frac{M}{2E} \right]^{1/2} . \quad (3)$$

In Eqs. (2) and (3), $E$ is the projectile ion energy in the laboratory frame, $m$ is the electron mass, and $M$ is the ionic mass.

The total dielectronic recombination cross section for an initial level $i$ is given by

$$\sigma_{\mathrm{DR}}(i) = \sum_j G(E_c, \Delta E) \bar{\sigma}(i \rightarrow j) , \quad (4)$$

where $G(E_c, \Delta E)$ is a Gaussian convolution integral cen-

 

tered at $E_c$ with an experimental energy resolution of $\Delta E > \Delta E_c$.

The many radiative and autoionization rates needed for the cross-section expressions of Eqs. (1) through (4) are calculated in a fully relativistic Dirac-Fock method. The computational approach is similar in spirit to the methods developed by Chen.[11] Energies and bound states wave functions are obtained using Grant *et al.*'s MCDF multiconfiguration Dirac-Fock atomic structure code.[12] Breit interaction and QED corrections to the energies and wave functions are also obtained using McKenzie, Grant, and Norrington's BENA code.[13]

The algebraic reduction for multielectron matrix elements involving one-body tensor operators is provided by Pyper, Grant, and Beatham's MCT code.[14] The resulting radiative single particle matrix elements are given by

$$M_r = \int d^4x \bar{\Psi}_1(x)\gamma^u A_u(x)\Psi_2(x) \ . \tag{5}$$

where $A_u(x)$ is the vector potential and $\Psi(x)$ is a single-particle wave function. We have developed a code labeled MCRAD to evaluate electric dipole transition amplitudes in the velocity or length gauges.

The algebraic reduction for multielectron matrix elements involving two-body tensor operators is provided by Grant's MCP code[15] and McKenzie *et al.*'s MCBP code.[13] The resulting autoionizing single-particle matrix elements are given by

$$M_a = \int d^4x \int d^4y \int d^4q \bar{\Psi}_1(x)\gamma_u \Psi_2(x) \frac{e^{-iq(x-y)}}{q^2+i\alpha} \times \bar{\Psi}_3(y)\gamma^u \Psi_4(y) \ , \tag{6}$$

where the Lorentz gauge has been chosen for the photon propagator. For autoionization, one of the $\Psi$'s in Eq. (6) represents a single-particle continuum wave function given by

$$\Psi(x) = \frac{1}{r} \begin{bmatrix} P_{\varepsilon\kappa}(r) & \phi_{\kappa m} \\ iQ_{\varepsilon\kappa}(r) & \phi_{-\kappa m} \end{bmatrix} , \tag{7}$$

where $\varepsilon$ is the total energy of the electron minus its rest energy, $\kappa = -2(j-l)(j+\frac{1}{2})$, and $\phi_{\kappa m}$ is an *lsj*-coupled spherical harmonic. The continuum radial orbitals are solutions to the single-channel Dirac equation:

$$\left[\frac{d}{dr} + \frac{\kappa}{r}\right] P_{\varepsilon\kappa}(r) + \frac{1}{c}(V - \varepsilon - 2c^2) Q_{\varepsilon\kappa}(r) = 0 \ , \tag{8}$$

$$\left[\frac{d}{dr} - \frac{\kappa}{r}\right] Q_{\varepsilon\kappa}(r) - \frac{1}{c}(V - \varepsilon) P_{\varepsilon\kappa}(r) = 0 \ , \tag{9}$$

where $V$ is the sum of the nuclear potential and the distorting potential constructed from previously calculated Dirac-Fock target orbitals, and $c$ is the speed of light. We have developed a code labeled MCAUTO to evaluate both Coulomb electrostatic and Breit retarded electromagnetic contributions to the autoionizing transition amplitude.

The radiative and autoionization rates for Eqs. (1)–(4) may also be evaluated in a configuration-mixing intermediate-coupling approximation using the previously developed AUTOSTRUCTURE code.[7,8] For application to highly charged ions, the existing code was modified in a manner following the work of Cowan and Griffin.[16] By solving Eq. (9) for $Q_{\varepsilon\kappa}$ and substituting into Eq. (8) the single-channel Dirac equation may be written as

$$\left[\frac{d^2}{dr^2} - \frac{l(l+1)}{r^2}\right] P_{\varepsilon\kappa}(r) + \left[\frac{(V-\varepsilon)^2}{c^2} - 2V + 2\varepsilon\right] P_{\varepsilon\kappa}(r) - \frac{dV}{dr}\left[V - \varepsilon - 2c^2\right]^{-1} \left[\frac{dP/dr}{P} + \frac{\kappa}{r}\right] P_{\varepsilon\kappa}(r) = 0 \ . \tag{10}$$

Since the AUTOSTRUCTURE code is designed around the SUPERSTRUCTURE code's[17] nonrelativistic configurations, $\{(n_i l_i)^{w_i}\}$, as opposed to relativistic subconfigurations, $\{(n_i l_i j_i)^{w_i}\}$, we replace the $\kappa/r$ term in Eq. (10) by its $(2j+1)$ weighted average of $-1/r$. Once the relativistic $P_{\varepsilon l}(r)$ function is obtained, a similar replacement of the $\kappa/r$ term in Eq. (9) allows a relativistic $Q_{\varepsilon l}(r)$ function to be obtained. The differential equations for all bound and continuum radial orbitals in the AUTOSTRUCTURE code were thus modified in the manner described. All the one- and two-body electrostatic matrix elements were calculated using the relativistic $P_{nl}(r)$ and $Q_{nl}(r)$ radial orbitals. No other two-body electromagnetic matrix elements were included.

In summary, we distinguish four methods for calculating radiative and autoionization rates for the RTEX and DR cross section expressions. The Dirac-Fock (DF) method included only two-body Coulomb electrostatic interactions in the calculation of energies, wave functions, and transition amplitudes. The Dirac-Fock Breit (DFB) method extends the DF method to include two-body Breit interaction and QED effects. Rates may also be calculated using the standard AUTOSTRUCTURE package (AS) as well as the new semirelativistic version (ASR).

## III. RESULTS

For resonant transfer and excitation in collisions of $U^{90+}$ with $H_2$, we considered the following reaction pathways:

$$U^{90+}(1s^2) + H_2 \rightarrow U^{89+}(1s2l2l') + H_2^+$$

$$U^{89+}(1s2l2l') \rightarrow \begin{cases} U^{90+}(1s^2) + e^- \\ U^{89+}(1s^2 2l'') + h\nu \ . \end{cases} \tag{11}$$

The radiative emission pathway is strongly preferred, thus the DR cross section of Eq. (1) is directly proportional to the relatively weak autoionization rate $A_a(j \rightarrow i)$. In Table I we present energies and autoionizing rates for the 16 possible $1s2l2l'$ resonances of the recombining ion $U^{89+}$ calculated using the fully relativis-

TABLE I. Energies and autoionizing rates for $U^{89+}$. Values in square brackets denote powers of ten.

| Level | DF method energy (Ry) | DF method rate (Hz) | DFB method energy (Ry) | DFB method rate (Hz) |
|---|---|---|---|---|
| $1s2s^2(1/2)$ | 4668 | 3.84[14] | 4635 | 6.26[14] |
| $1s2s(1)2\bar{p}(1/2)$ | 4672 | 1.55[12] | 4640 | 2.47[14] |
| $1s2s(1)2\bar{p}(3/2)$ | 4677 | 1.43[13] | 4638 | 1.42[13] |
| $1s2s(0)2\bar{p}(1/2)$ | 4689 | 5.30[14] | 4659 | 8.25[14] |
| $1s2\bar{p}^2(1/2)$ | 4698 | 4.97[12] | 4663 | 2.25[12] |
| $1s2s(1)2p(5/2)$ | 4991 | | 4952 | 9.40[11] |
| $1s2s(1)2p(3/2)$ | 4998 | 3.68[12] | 4960 | 2.18[12] |
| $1s2s(1)2p(1/2)$ | 5003 | 4.40[13] | 4966 | 3.25[12] |
| $1s2s(0)2p(3/2)$ | 5009 | 1.34[14] | 4976 | 2.06[14] |
| $1s2\bar{p}(0)2p(3/2)$ | 5010 | 9.80[12] | 4973 | 5.72[13] |
| $1s2\bar{p}(1)2p(5/2)$ | 5014 | 1.07[14] | 4971 | 1.11[14] |
| $1s2\bar{p}(1)2p(1/2)$ | 5015 | 3.11[12] | 4976 | 1.75[13] |
| $1s2\bar{p}(1)2p(3/2)$ | 5016 | 1.60[14] | 4982 | 7.69[13] |
| $1s2p^2(2)(5/2)$ | 5331 | 4.52[13] | 5290 | 6.92[13] |
| $1s2p^2(2)(3/2)$ | 5335 | 3.36[13] | 5297 | 1.01[13] |
| $1s2p^2(0)(1/2)$ | 5338 | 1.84[13] | 5300 | 4.02[13] |

tic Dirac-Fock method. Breit interaction and QED effects generally lower the resonance energies by about 35 Ry. The Breit interaction has a significant effect on most of the autoionization rates found in Table I, more often than not increasing the rates although there is no systematic trend. The $1s2p^2(2)(3/2)$ rate, for example, is found to decrease by a factor of 3. Here, the parentheses denote the $j$ values of the subconfigurations and the coupling order. In Fig. 1 we present the *KLL* RTEX cross section versus projectile rest-frame energy for $U^{90+}$ collisions with $H_2$; multiply by $M/m$ to obtain the projectile energy in the laboratory frame (see Sec. II). Since the $2s(j=1/2)$ and $2\bar{p}(j=1/2)$ orbitals have nearly the same single-particle energy, the resonance levels fall into three main energy groups which give rise to the three peaks found in Fig. 1. The Breit interaction has a significant effect only on the lowest energy resonance peak involving the $1s2s^2$, $1s2s2\bar{p}$, and $1s2\bar{p}^2$ subconfigurations.

In Fig. 2 we present the *KLL* RTEX cross section versus energy for $U^{90+}$ collisions with $H_2$ calculated using the AUTOSTRUCTURE code. Substantial changes are found in resonance energies and peak heights when the standard method is modified to include direct relativistic effects on radial orbitals. In fact the ASR cross-section results of Fig. 2 are in good agreement with the Dirac-Fock results of Fig. 1. One of the main conclusions of the paper is that the Dirac-Fock method and the modified AUTOSTRUCTURE code give similar cross-section results.

For resonant transfer and excitation in collisions of $U^{89+}$ with $H_2$, we considered the following reaction pathways:

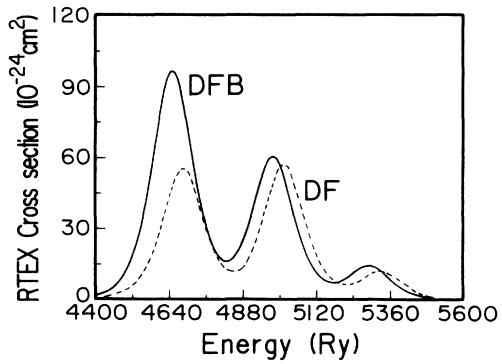


FIG. 1. RTEX cross section for $U^{90+}$ collisions with $H_2$ as a function of projectile energy times $m/M$. Solid curve, Dirac-Fock method with Breit interaction corrections; dashed curve, Dirac-Fock method.

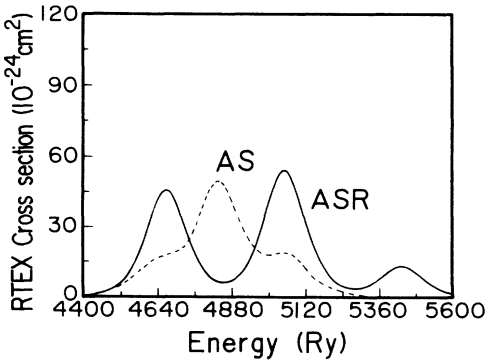


FIG. 2. RTEX cross section for $U^{90+}$ collisions with $H_2$ as a function of projectile energy times $m/M$. Solid curve, AUTOSTRUCTURE with relativistic corrections; dashed curve, AUTOSTRUCTURE.

$$U^{89+}(1s^2 2s)+H_2 \rightarrow U^{88+}(1s2l2l'2l'')+H_2^+$$

$$U^{88+}(1s2l2l'2l'') \rightarrow \begin{cases} U^{89+}(1s^2 2l''')+e^- \\ U^{88+}(1s^2 2l'''2l'''')+h\nu \end{cases} \quad (12)$$

The radiative emission pathway is again strongly preferred, thus the DR cross section of Eq. (1) is proportional to the autoionization rate. In Fig. 3 we present the *KLL* RTEX cross section versus energy for $U^{89+}$ collisions with $H_2$ calculated using the Dirac-Fock method with Breit interaction corrections (DFB) and the modified AUTOSTRUCTURE code (ASR). Due to the near degeneracy of the $2s$ and $2\bar{p}$ orbitals, the 30 possible $1s2l2l'2l''$ resonances of $U^{88+}$ fall into three main energy groups corresponding to the three peaks found in Fig. 3. A comparison of the calculational results indicates that Breit interaction effects are large for the lowest-energy peak involving the $1s2s^2 2\bar{p}$ and $1s2s2\bar{p}^2$ subconfigurations. Our Dirac-Fock method with Breit interaction results for the *KLL* resonances of $U^{89+}$ are in very good agreement with a similar calculation by Chen.[18] The modified AUTOSTRUCTURE code results are also in good agreement with Chen's Dirac-Fock calculations. For the dielectronic recombination of $U^{89+}$ we considered the following reaction pathways:

$$e^- + U^{89+}(1s^2 2s) \leftrightarrows U^{88+}(1s^2 2p6l) \rightarrow \begin{cases} U^{89+}(1s^2 2\bar{p})+e^- \\ U^{88+}(1s^2 2s6l)+h\nu_1 \\ U^{88+}(1s^2 2pnl')+h\nu_2 \end{cases} \quad (13)$$

The radiative and autoionizing pathways are found to be roughly comparable for outer shell $\Delta n=0$ dielectronic recombination in $U^{89+}$. The $U^{89+}2s(1/2)-2p(3/2)$ energy separation obtained with the ASR code was 382 Ry compared to 328 Ry obtained from the DFB calculation. Consequently, the continuum was lowered by 54 Ry in the ASR calculation of the $\Delta n=0$ DR cross sections. The remaining difference in the $n=6$ resonance energies is then due explicitly to the different treatments of the $n=6$ orbitals (see Sec. II). In Fig. 4 we present the $n=6$ DR cross section versus energy for $U^{89+}$ calculated using the Dirac-Fock method with Breit corrections and the modified AUTOSTRUCTURE code. The cross section is convoluted with a 5.0-Ry experimental energy distribution. The $1s^2 2p6l$ resonances of $U^{88+}$ fall into two main energy groups corresponding to the two peaks found in Fig. 4. The lowest-energy peak only involves the $1s^2 2p6s$ and $1s^2 2p6\bar{p}$ subconfigurations. The two calculational methods agree well in size and shape of the resonance structures, indicating that the overall effect of the Breit interaction is small.

In Fig. 5 we present the DR cross section versus energy for $U^{89+}$ calculated using the modified AUTOSTRUCTURE code. The cross section is convoluted with a 5.0-Ry experimental energy distribution and includes contributions from all $1s^2 2pnl$ subconfigurations of $U^{88+}$.

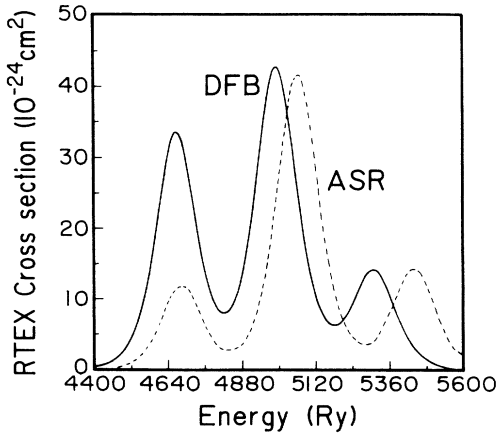


FIG. 3. RTEX cross section for $U^{89+}$ collisions with $H_2$ as a function of projectile energy times $m/M$. Solid curve, Dirac-Fock method with Breit interaction corrections; dashed curve, AUTOSTRUCTURE with relativistic corrections.

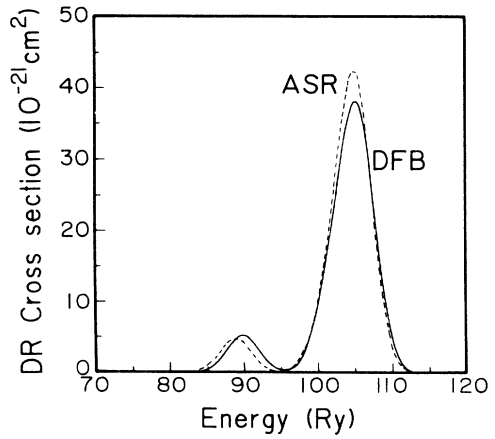


FIG. 4. DR cross section for $U^{89+}$ as a function of incident electron energy. Solid curve, Dirac-Fock method with Breit interaction corrections; dashed curve, AUTOSTRUCTURE with relativistic corrections.

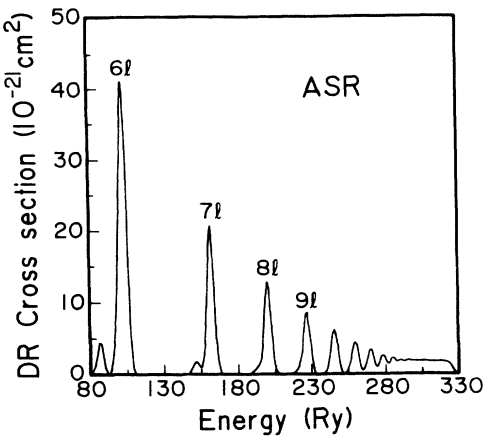


FIG. 5. DR cross section for $U^{89+}$ as a function of incident electron energy. Solid curve, AUTOSTRUCTURE with relativistic corrections.

## IV. SUMMARY

We have employed a fully relativistic Dirac-Fock method to calculate RTEX and DR cross sections for highly charged uranium ions. We have found that the cross sections calculated using the DF method are in good agreement with these calculated using a modified version of the AUTOSTRUCTURE code in which bound and continuum relativistic *nl* radial orbitals are used to evaluate one- and two-body electrostatic matrix elements. When the Dirac-Fock method is extended to include Breit interactions, the lower energy peaks in the *K*-shell-vacancy RTEX cross sections are significantly enhanced. Breit interaction effects on the *L*-shell-vacancy DR cross sections are found to be negligible.

## ACKNOWLEDGMENTS

We wish to thank M. H. Chen and D. C. Griffin for useful discussions on relativistic atomic structure and W. G. Graham and A. Müller for comments on future heavy-ion experiments. This work was supported by the Office of Fusion Energy, U.S. Department of Energy, under Contract No. DE-FG05-86-ER53217 with Auburn University.

[1]Proceedings of the Workshop on Highly Charged Ions: New Physics and Advanced Techniques, Berkeley, 1989 [Nucl. Instrum. Methods Phys. Res. B **43**, 265 (1989)].
[2]W. G. Graham, K. H. Berkner, E. M. Bernstein, M. W. Clark, B. Feinberg, M. A. McMahan, T. J. Morgan, W. Rathbun, A. S. Schlacter, and J. A. Tanis (unpublished).
[3]A. Müller (private communication).
[4]D. Brandt, Phys. Rev. A **27**, 1314 (1983).
[5]Y. Hahn, Phys. Rev. A **40**, 2950 (1989).
[6]I. P. Grant and H. M. Quiney, Adv. At. Mol. Phys. **23**, 37 (1988).
[7]N. R. Badnell, J. Phys. B **19**, 3827 (1986).
[8]N. R. Badnell and M. S. Pindzola, Phys. Rev. A **39**, 1685 (1989).
[9]Y. Hahn, Adv. At. Mol. Phys. **21**, 123 (1985).
[10]J. S. Lee, J. Chem. Phys. **66**, 4906 (1977).
[11]M. H. Chen, Phys. Rev. A **31**, 1449 (1985).
[12]I. P. Grant, B. J. McKenzie, P. H. Norrington, D. F. Mayers, and N. C. Pyper, Comput. Phys. Commun. **21**, 207 (1980).
[13]B. J. McKenzie, I. P. Grant, and P. H. Norrington, Comput. Phys. Commun. **21**, 233 (1980).
[14]N. C. Pyper, I. P. Grant, and N. Beatham, Comput. Phys. Commun. **15**, 387 (1978).
[15]I. P. Grant, Comput. Phys. Commun. **5**, 263 (1973).
[16]R. D. Cowan and D. C. Griffin, J. Opt. Soc. Am. **66**, 1010 (1976).
[17]W. Eissner, M. Jones, and H. Nussbaumer, Comput. Phys. Commun. **8**, 270 (1974).
[18]M. H. Chen, Phys. Rev. A **41**, 4102 (1990).